Letter | Editors' Suggestion

Bipolaronic superconductivity out of a Coulomb gas

J. Sous,[1,2,*,†] C. Zhang,[3,*,‡] M. Berciu,[4,5] D. R. Reichman,[6] B. V. Svistunov,[7,8] N. V. Prokof'ev,[7] and A. J. Millis[9,10,§]

[1]*Department of Physics, Stanford University, Stanford, California 93405, USA*
[2]*Stanford Institute for Theoretical Physics, Department of Physics, Stanford University, Stanford, California 93405, USA*
[3]*Department of Modern Physics, University of Science and Technology of China, Hefei, Anhui 230026, China and Hefei National Laboratory, University of Science and Technology of China, Hefei, Anhui 230088, China*
[4]*Department of Physics and Astronomy, University of British Columbia, Vancouver, British Columbia, Canada V6T 1Z1*
[5]*Stewart Blusson Quantum Matter Institute, University of British Columbia, Vancouver, British Columbia, Canada V6T 1Z4*
[6]*Department of Chemistry, Columbia University, New York, New York 10027, USA*
[7]*Department of Physics, University of Massachusetts, Amherst, Massachusetts 01003, USA*
[8]*Wilczek Quantum Center, School of Physics and Astronomy and T. D. Lee Institute, Shanghai Jiao Tong University, Shanghai 200240, China*
[9]*Department of Physics, Columbia University, New York, New York 10027, USA*
[10]*Center for Computational Quantum Physics, Flatiron Institute, 162 5th Avenue, New York, New York 10010, USA*

(Received 4 December 2022; revised 2 July 2023; accepted 6 November 2023; published 13 December 2023)

Employing an unbiased sign-problem-free quantum Monte Carlo approach, we investigate the effects of long-range Coulomb forces on Bose-Einstein condensation of bipolarons using a model of bond phonon-modulated electron hopping. In the absence of long-range repulsion, this model was recently shown to give rise to small-size light-mass bipolarons that undergo a superfluid transition at high values of the critical transition temperature T_c. We find that T_c in our model, even with the long-range Coulomb repulsion, remains much larger than that of Holstein bipolarons and can be on the order of or greater than the typical upper bounds on phonon-mediated T_c based on the Migdal-Eliashberg and McMillan approximations. Our work points to a physically simple mechanism for superconductivity in the low-density regime that may be relevant to current experiments on dilute superconductors.

DOI: 10.1103/PhysRevB.108.L220502

Introduction. Understanding the mechanisms of superconductivity in the dilute density regime is an active theme of research, relevant to a large and growing list of ultralow-carrier-density superconductors including polar materials [1,2], doped topological insulators [3,4], transition-metal dichalcogenides [5], moiré materials [6–11], and other materials [12] where, as a matter of principle, the Fermi-liquid/Migdal-Eliashberg paradigm must fail. Bose-Einstein condensation (BEC) of preformed pairs (bipolarons) in principle offers a robust route to superconductivity at low densities. However, in the low-density regime, the Coulomb repulsion is weakly screened and thus the pairing "glue" required to bind electron pairs into bound states must be strong enough to overcome the Coulomb repulsion. A strong pairing interaction is usually believed to result in heavy bound states, implying low values of the critical transition temperature T_c [13,14]; however, we have recently shown [15] that electrons coupled to phonons via bond phonon-modulated electron hopping form small-size light-mass bipolarons [16,17] that undergo a superfluid (BEC) transition at values of T_c that, even in the presence of a large on-site Hubbard repulsion U, are much larger than those obtained in density-coupled (Holstein) models or from Migdal-Eliashberg theory. However, previous literature on bipolaronic (and other nonphononic BEC [18–22]) mechanisms for superconductivity deals only with short-range interactions, neglecting the long-range part of the Coulomb interaction, and so is not directly applicable to ungated two-dimensional (2D) materials or 3D materials in which the Coulomb repulsion cannot be screened by an external gate.

In this Letter, we study pairing and BEC of bond-coupled bipolarons occurring in a dilute 3D Coulomb gas, showing that its T_c is higher than that of density-coupled (Holstein) bipolarons and in line with experimental values of T_c found in 3D materials believed to be close to or in the low-density regime (see Fig. 1). This subject has been treated using different approximations [13,23,24] and the physics has remained subject to debate. Our theory uses a numerically exact, unbiased method that takes the long-ranged Coulomb interaction into account and (i) demonstrates a realistic mechanism for BEC formation at relatively high values of T_c and (ii) reveals the properties of bipolarons, e.g., their mass and size, in three dimensions.

Model. We consider the bond-Peierls [25] (or bond–Su-Schrieffer-Heeger [26]) electron-phonon coupling on a 3D cubic lattice. In this model the electronic hopping between two sites is modulated by a single oscillator centered on the bond connecting the two sites [15]. The Hamiltonian is

$$\hat{\mathcal{H}} = \hat{\mathcal{H}}_e + \hat{\mathcal{H}}_{ph} + \hat{\mathcal{V}}_{e\text{-}ph}. \quad (1)$$

*These authors contributed equally to this work.
†Present address: Department of Chemistry and Biochemistry, University of California, San Diego, La Jolla, California 92093, USA.
‡Author to whom correspondence should be addressed: zhangchao1986sdu@gmail.com
§Author to whom correspondence should be addressed: ajm2010@columbia.edu

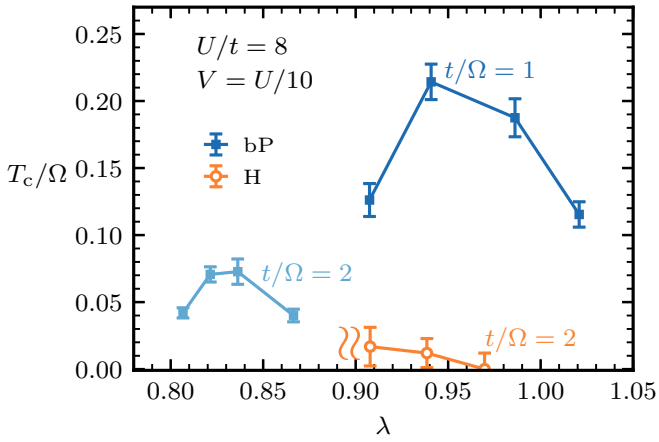

FIG. 1. Estimates of T_c of the bond-Peierls (bP) bipolaronic superconductor (closed squares, blue lines) for different t/Ω at $U = 8t$ and $\mathcal{V}_{r>0} = V/r$, with $V = U/10$, as a function of λ computed according to Eq. (3) from QMC simulations of the bipolaron effective mass $m^\star_{\rm BP}$ and its mean-square radius $R^2_{\rm BP}$, contrasted with superconductivity of Holstein (H) bipolarons (open circles, orange line) at $t/\Omega = 2$ for the same values of U/t and V. Here we define $\lambda = \alpha^2/3\Omega t$ for bond-Peierls bipolarons and $\lambda = 0.85\alpha^2/6\Omega t$ for Holstein bipolarons. The doubly wavy symbol indicates the absence of bipolarons in the Holstein model for $\lambda \lesssim 0.91$ where a crossover from BEC to the BCS regime may occur.

Here the lattice Coulomb model for electrons with spin $\sigma \in \{\uparrow, \downarrow\}$ is $\hat{\mathcal{H}}_e = -t\sum_{\langle i,j\rangle,\sigma}(\hat{c}^\dagger_{i,\sigma}\hat{c}_{j,\sigma} + \text{H.c.}) + U\sum_i \hat{n}_{i,\uparrow}\hat{n}_{i,\downarrow} + \frac{1}{2}\sum_{i\neq j}\mathcal{V}_{i,j}\hat{n}_i\hat{n}_j$, with nearest-neighbor (NN) hopping t, on-site Hubbard repulsion U, NN repulsion V, and longer-range repulsion $\mathcal{V}_{ij} = \frac{Va}{|r_i - r_j|}$, where $\hat{n}_i = \hat{n}_{i,\uparrow} + \hat{n}_{i,\downarrow}$, with $\hat{n}_{i,\sigma} = \hat{c}^\dagger_{i,\sigma}\hat{c}_{i,\sigma}$ at site r_i, and a is the lattice constant (NN distance). The notation $\langle i, j\rangle$ refers to NN sites. We estimate the on-site $U = e^2/\epsilon a_{\rm orb}$, with $a_{\rm orb}$ the unit cell orbital size and ϵ a background dielectric constant, the NN $V = e^2/\epsilon a \approx U a_{\rm orb}/a$, and further-neighbor (distance $r > a$) $\mathcal{V}_{r>a} = Va/r$. We henceforth set the lattice constant $a = 1$. We model distortions of the bonds connecting sites i and j as Einstein oscillators with the Hamiltonian $\hat{\mathcal{H}}_{\rm ph} = \sum_{\langle i,j\rangle}(\frac{1}{2}K\hat{X}^2_{i,j} + \hat{P}^2_{i,j}/2M) = \Omega\sum_{\langle i,j\rangle}\hat{b}^\dagger_{i,j}\hat{b}_{i,j}$ with oscillator frequency ($\hbar = 1$) $\Omega = \sqrt{K/M}$. The interaction between electrons and phonons takes the form

$$\hat{\mathcal{V}}_{\text{e-ph}} = \alpha\sqrt{2M\Omega}\sum_{\langle i,j\rangle,\sigma}(\hat{c}^\dagger_{i,\sigma}\hat{c}_{j,\sigma} + \text{H.c.})\hat{X}_{i,j}, \qquad (2)$$

describing the modulation of electron hopping by an oscillator $\hat{X}_{i,j} := \frac{1}{\sqrt{2M\Omega}}(\hat{b}^\dagger_{i,j} + \hat{b}_{i,j})$ associated with the bond connecting sites i and j with coupling coefficient $\alpha\sqrt{2M\Omega}$. We set $M = 1$. The relevant parameters are a dimensionless coupling constant $\lambda = [(\alpha\sqrt{2\Omega})^2/K]/6t = \alpha^2/3\Omega t$, the ratio of the typical polaronic energy scale to the free-electron energy scale, and an adiabaticity parameter t/Ω. It is important to note that a typical physical origin for this phonon-modulated hopping is from interference of different hopping pathways [15]. This means that the model remains valid even when the lattice displacement is large enough that the electronic hopping changes sign. This is different from other models of phonon-modulated

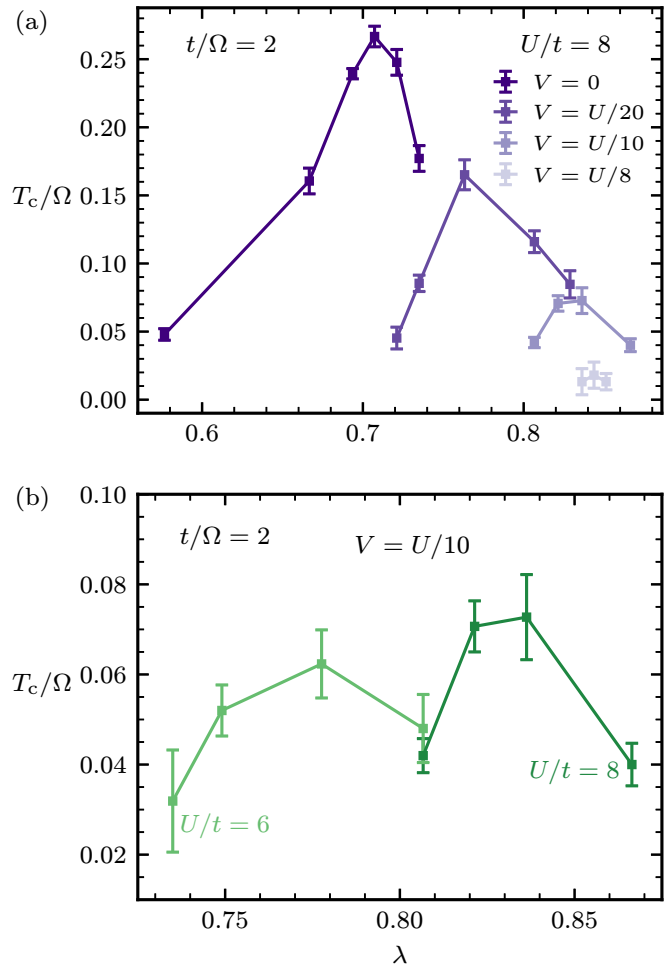

FIG. 2. Estimates of T_c of the bond-Peierls bipolaronic superconductor for $t/\Omega = 2$ as a function of $\lambda = \alpha^2/3\Omega t$ for (a) different strengths of the Coulomb repulsion V at fixed on-site $U/t = 8$ and (b) different strengths of the on-site U at fixed long-range repulsion $V = U/10$, computed according to Eq. (3) from QMC simulations of the bipolaron effective mass $m^\star_{\rm BP}$ and mean-square radius $R^2_{\rm BP}$.

hopping [16,27–31] in which an equation of the general form of Eq. (2) applies only in the small-displacement regime where the net change in hopping amplitude is small relative to the bare hopping [32].

Method. Using a numerically exact sign-problem-free quantum Monte Carlo (QMC) approach based on a path-integral formulation of the electronic sector combined with either a real-space diagrammatic or a Fock-space path-integral representation of the phononic sector [17], we study singlet bipolaron formation in the two-electron sector of the model. Technical details about the QMC methodology can be found in Refs. [15,17]. For reference, QMC methods were previously used to study the model at half filling in two dimensions in a number of works [33–37]. Here we simulate the model on a 3D cubic lattice with linear size $L = 140$ sites and open boundary conditions. This system size is large enough to access the thermodynamic limit and eliminate boundary effects. We simulate the behavior of the model for two values of $t/\Omega = 1, 2$. Values of t/Ω larger than 2 present a computational challenge. Both of these values of Ω are much smaller

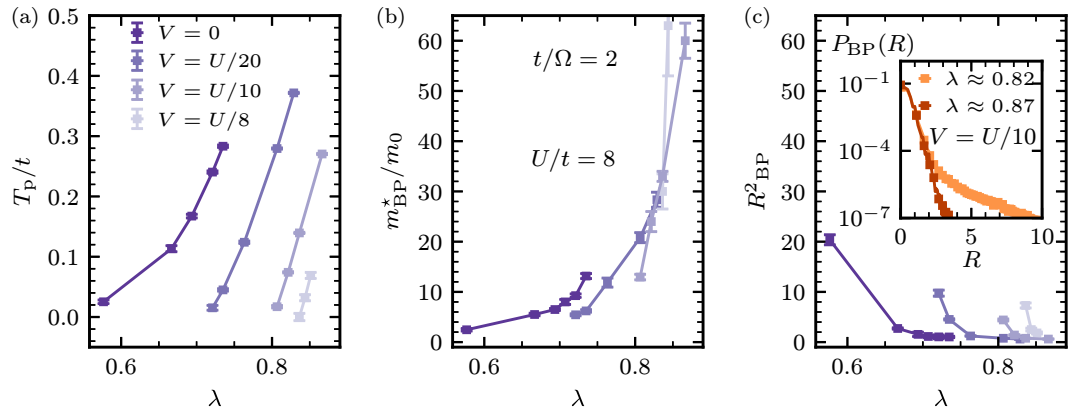

FIG. 3. Bipolaron properties in the model (1) at $t/\Omega = 2$ as a function of $\lambda = \alpha^2/3\Omega t$ for different V at fixed $U/t = 8$: (a) bipolaron binding energy T_p, (b) bipolaron effective mass $m^\star_{BP}$ in units of the mass of two free electrons $m_0 = 2m_e = 1/t$, and (c) bipolaron square radius R^2_{BP} and, in the inset, its radial size probability density distribution $P_{BP}(R)$ (probability distribution of finding the two electrons within a bound bipolaron at a distance R from their center-of-mass position) at large coupling for $V = U/10$. Error bars in $P_{BP}(R)$ correspond to statistical errors smaller than the symbol size and therefore are not shown.

than the bare electronic bandwidth in three dimensions ($12t$), thus serving as representative values for the adiabatic limit of slow phonons. In what follows we focus primarily on results for this value of $t/\Omega = 2$; the $t/\Omega = 1$ case is similar.

BEC of bipolarons. In three dimensions, a dilute system of electrons, at strong enough electron-phonon coupling, is unstable to the formation of bipolarons and thus forms a gas of interacting bosons. Competing instabilities such as phase separation [38] or Wigner crystallization [39] may occur only when the density is extremely low. Thus, based on recent results on BEC out of a Coulomb Bose plasma [40], bipolarons will undergo condensation into a BEC and superfluidity at a $T \leqslant T_c$, with $T_c \approx 3.2\rho_{BP}^{2/3}/m^\star_{BP}$, where ρ_{BP} is the density of bipolarons and $m^\star_{BP} := \{[\partial^2 E_{BP}(K)/\partial K^2]|_{K=0}\}^{-1}$ is the bipolaron effective mass, with $E_{BP}(K)$ the bipolaron dispersion and K the bipolaron momentum. This estimate remains reliable in a broad density range up to the density at which bipolarons overlap. The largest T_c from this mechanism is thus expected to arise around the density $\rho_{BP} = \min[1/(\frac{4}{3}\pi R^3_{BP}), 1/(\frac{4}{3}\pi)]$ at which the interparticle separation becomes on the order of the bipolaron radial size R_{BP}, which, after lattice regularization, must be at least unity. This leads to an estimate of T_c of the bipolaron superconductor at the overlap density that depends only on the bipolaron properties given by

$$T_c \approx \begin{cases} \frac{1.2}{m^\star_{BP} R^2_{BP}} & \text{if } R^2_{BP} \geqslant 1 \\ \frac{1.2}{m^\star_{BP}} & \text{otherwise,} \end{cases} \tag{3}$$

where $R^2_{BP} := \langle \Psi_{BP}|\hat{R}^2|\Psi_{BP}\rangle$ is the bipolaron mean-square radius, with Ψ_{BP} the bipolaron ground-state wave function.

Bipolaronic superconductivity out of a Coulomb gas. Figure 1 presents T_c/Ω computed from Eq. (3) using $m^\star_{BP}$ and R^2_{BP} obtained from QMC simulations as a function of λ for different t/Ω at $U = 8t$ and $V = U/10$. Error bars in the figures represent one standard deviation statistical errors in QMC simulations. The reentrant behavior (increase and then decrease) of the optimal T_c as a function of λ observed in Fig. 1 results from a competition between the increase in mass and decrease in radius of the bipolarons as λ is increased (see Ref. [15]). Figure 1 shows that a sufficiently large value of λ is needed in three dimensions in order to form bound states and obtain an s-wave bipolaronic superconductor in the regime of strong correlations. Our choice of $U/t = 8$ implies strong competition between the on-site repulsion and the electronic kinetic energy and the ratio $V/U = 1/10$ is a reasonable estimate for most materials (e.g., transition-metal oxides), with a roughly 10:1 ratio between the lattice constant (approximately 4 Å) and the orbital size (approximately 0.5 Å). Thus, our results in Fig. 1 prove that bipolaronic superconductivity is robust even in the presence of strong, poorly screened Coulomb repulsion. To appreciate this result, we contrast in Fig. 1 T_c/Ω with the superconducting transition-temperature of Holstein bipolarons [41,42] (with electron-phonon coupling $\hat{\mathcal{V}}_{e\text{-ph}} = \alpha\sqrt{2\Omega}\sum_{i,\sigma}\hat{c}^\dagger_{i,\sigma}\hat{c}_{i,\sigma}\hat{X}_i$), which is found to be always smaller. The values of T_c/Ω of the bond bipolarons also appear to be comparable to or greater than the upper bound of 0.05 from McMillan's phenomenological approach to Migdal-Eliashberg theory in the adiabatic limit for moderate values of $\lambda \lesssim 1$.[1] In other words, our theory predicts values of T_c in line with typical values found in experiments on dilute superconductors.

Figure 2 presents the dependence of T_c/Ω on V/U at fixed U/t [Fig. 2(a)] and on U/t at fixed V/U [Fig. 2(b)]. We find long-range repulsion-induced reduction of T_c, but T_c/Ω remains relatively large even for large $V = U/10$. This reflects the ability of the bipolaron wave function to spread itself effectively over multiple sites in order to accommodate the Coulomb repulsion [see the inset of Fig. 3(c)]. However, the on-site repulsion can enhance T_c similarly to what we found in 2D models with no long-range interaction [15]. This unconventional behavior follows from the ability of the bipolaron to reduce its mass without significantly increasing its radius as

[1]The McMillan formula [43] $\frac{T_c}{\Omega} = \frac{1}{1.45}\exp(-1.04\frac{1+\lambda}{\lambda-\mu^\star(1+0.62\lambda)})$ (where $\mu^\star = 0.12$ is the value of the Coulomb pseudopotential found in many materials) predicts a typical upper bound of $T_c/\Omega \sim 0.05$ at $\lambda = 1$.

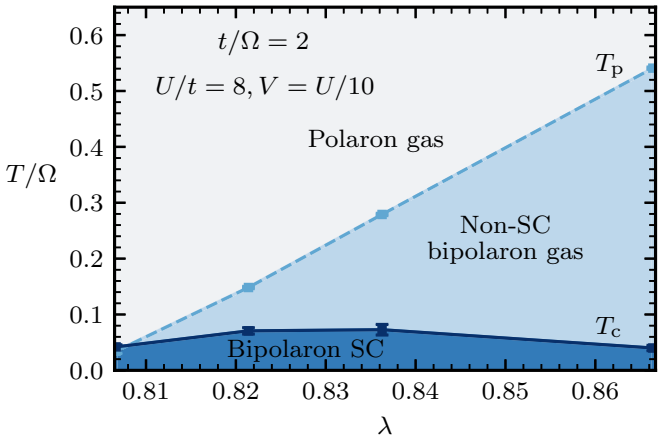

FIG. 4. Phase diagram in the T/Ω-λ space of the bond-Peierls model in the adiabatic limit $t/\Omega = 2$ with strong on-site $U/t = 8$ and Coulomb $V = U/10$ interactions. A BEC superconductor forms at $T \leqslant T_c$ (dark blue region). There is a large region at temperatures $T_c < T \leqslant T_p$ characterized by nonsuperconducting correlations and phase fluctuations in a normal gas of bipolarons (light blue region). Above T_p, the bipolarons unbind into a polaron gas (gray region).

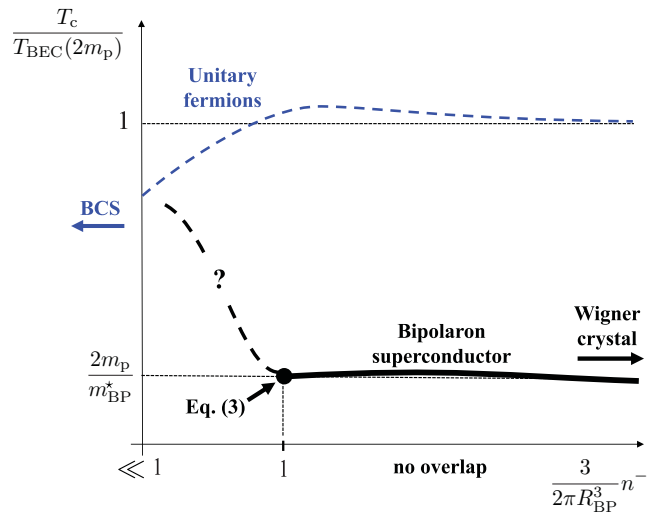

FIG. 5. The heavy black line shows the superfluid transition temperature T_c of the bipolaronic gas normalized to the BEC temperature T_{BEC} of a gas of bosons of density n and mass $2m_p$ as a function of the inverse density n^{-1} normalized to the effective bipolaron density $3/2\pi R^3_{BP}$. The black dashed line shows the proposed extrapolation of T_c beyond the density at which the bipolarons overlap (black dot) and the BEC picture breaks down. As the density enters the $n > 3/2\pi R^3_{BP}$ BCS regime we expect, based on comparison to the unitary Fermi gas (blue dashed line), that the decrease in mass associated with unbinding of bipolarons into Fermi-liquid quasiparticles may drive a further increase in T_c.

U is increased. Our analysis proves that the bond bipolaronic superconductivity is generally much less sensitive to Coulomb repulsion than Holstein bipolarons and can in fact take advantage of the local repulsion to increase T_c.

Phenomenology of bipolaronic superconductivity. Figure 3 details the features of bipolarons in the presence of long-range Coulomb repulsion. A much sharper dependence on the electron-phonon coupling becomes apparent for larger values of V, as can be seen in the pairing temperature (bipolaron binding energy, i.e., energy of the two-electron bound state relative to the lower-energy edge of the two-polaron continuum) T_p [Fig. 3(a)], effective mass [Fig. 3(b)], and square radius [Fig. 3(c)]. This behavior implies that breakdown of Fermi-liquid theory due to bipolaronic collapse depends nontrivially on the interplay of electron-phonon and electron-electron interactions and goes beyond the current understanding of the breakdown of Migdal-Eliashberg theory due to a first-order transition or crossover driven by bipolaron formation [44–52]. Further, Fig. 3(b) demonstrates that mass enhancement remains moderate. We can see from Figs. 3(b) and 3(c) that small-size bipolarons with $R_{BP} < 3$ exhibit rather weak mass enhancement $m^\star_{BP} < 10$, explaining the large values of T_c at optimized λ despite the strong Coulomb repulsion. The modest reduction in T_c found for $V = U/10$ means that it remains relatively high compared to expectations based on standard models, highlighting the ability of the bipolarons to tolerate the long-range Coulomb repulsion.

In Fig. 4 we present the phase diagram of the bipolaronic superconductor in the T-λ space in the adiabatic limit for large Coulomb repulsion. There is an extended region at temperatures $T_c < T \leqslant T_p$ characterized by nonsuperconducting correlations in a normal gas of bipolarons, which will give rise to a large regime of phase fluctuations in experiment. Above T_p, the bipolarons unbind into a polaron gas. Finally, in Fig. 5 we discuss the crossover or phase transition occurring as the density is increased into the BCS regime [53,54] in which bipolarons overlap. A useful analogy is provided by the unitary Fermi gas (fermions in the continuum interacting with attractive contact interaction) picture of the BCS-BEC crossover [55,56], where in the dilute limit weakly bound fermion pairs with mass twice the bare fermion mass condense into a BEC and as the density is increased into the BCS regime of overlapping pairs T_c drops only slowly. The basic physics of the BCS-BEC crossover in the bipolaron system should be similar to that for unitary fermions but with the additional feature that the mass drops rapidly as the density increases beyond the point at which bipolarons overlap and unbind into polarons (with mass m_p) and then into moderately renormalized electrons. This density dependence of the mass, not present in the unitary Fermi gas, may lead to a further increase in T_c as the density is increased into the BCS regime.

Conclusion. We have shown that the local on-site Coulomb repulsion enhances T_c while the nonlocal part reduces T_c, which however remains relatively high. The key ingredient of the combination of light mass and relatively small size of bipolarons even in the presence of long-range Coulomb repulsion explains the robustness of the mechanism and the relatively large values of T_c found. The crossover or phase transition to the BCS regime when bipolarons start to overlap is an open question, but, in contrast to the unitary Fermi gas [55,56], we cannot rule out that T_c may have a peak as a function of carrier density in the crossover region where bipolarons unbind into quasiparticles with much smaller mass, which would imply even larger values of T_c on the BCS side.

Acknowledgments. We acknowledge useful discussions with S. Kivelson and S. Raghu. J.S. acknowledges support

from the Gordon and Betty Moore Foundation's EPiQS Initiative through Grant No. GBMF8686 at Stanford University. J.S., D.R.R., and A.J.M. acknowledge support from the National Science Foundation (NSF) Materials Research Science and Engineering Centers program through Columbia University in the Center for Precision Assembly of Superstratic and Superatomic Solids under Grant No. DMR-1420634. C.Z. acknowledges support by the National Natural Science Foundation of China (NSFC) under Grants No. 12204173 and No. 12275263, and the Innovation Program for Quantum Science and Technology (under Grant No. 2021ZD0301900). M.B. acknowledges support from the Natural Sciences and Engineering Research Council of Canada, the Stewart Blusson Quantum Matter Institute, and the Max-Planck-UBC-UTokyo Center for Quantum Materials. B.V.S. and N.V.P acknowledge support from the NSF under Grant No. DMR-2032077. J.S. also acknowledges the hospitality of the Center for Computational Quantum Physics at the Flatiron Institute. The Flatiron Institute is a division of the Simons Foundation.

[1] J. F. Schooley, W. R. Hosler, and M. L. Cohen, Superconductivity in semiconducting $SrTiO_3$, Phys. Rev. Lett. **12**, 474 (1964).

[2] M. N. Gastiasoro, J. Ruhman, and R. M. Fernandes, Superconductivity in dilute $SrTiO_3$: A review, Ann. Phys. (NY) **417**, 168107 (2020).

[3] V. Fatemi, S. Wu, Y. Cao, L. Bretheau, Q. D. Gibson, K. Watanabe, T. Taniguchi, R. J. Cava, and P. Jarillo-Herrero, Electrically tunable low-density superconductivity in a monolayer topological insulator, Science **362**, 926 (2018).

[4] E. Sajadi, T. Palomaki, Z. Fei, W. Zhao, P. Bement, C. Olsen, S. Luescher, X. Xu, J. A. Folk, and D. H. Cobden, Gate-induced superconductivity in a monolayer topological insulator, Science **362**, 922 (2018).

[5] T. Asaba, Y. Wang, G. Li, Z. Xiang, C. Tinsman, L. Chen, S. Zhou, S. Zhao, D. Laleyan, Y. Li, Z. Mi, and L. Li, Magnetic field enhanced superconductivity in epitaxial thin film WTe_2, Sci. Rep. **8**, 6520 (2018).

[6] Y. Cao, V. Fatemi, S. Fang, K. Watanabe, T. Taniguchi, E. Kaxiras, and P. Jarillo-Herrero, Unconventional superconductivity in magic-angle graphene superlattices, Nature (London) **556**, 43 (2018).

[7] X. Lu, P. Stepanov, W. Yang, M. Xie, M. A. Aamir, I. Das, C. Urgell, K. Watanabe, T. Taniguchi, G. Zhang, A. Bachtold, A. H. MacDonald, and D. K. Efetov, Superconductors, orbital magnets and correlated states in magic-angle bilayer graphene, Nature (London) **574**, 653 (2019).

[8] M. Yankowitz, S. Chen, H. Polshyn, Y. Zhang, K. Watanabe, T. Taniguchi, D. Graf, A. F. Young, and C. R. Dean, Tuning superconductivity in twisted bilayer graphene, Science **363**, 1059 (2019).

[9] G. Chen, A. L. Sharpe, P. Gallagher, I. T. Rosen, E. J. Fox, L. Jian, B. Lyu, H. Li, K. Watanabe, T. Taniguchi, J. Jung, Z. Shi, D. Goldhaber-Gordo, Y. Zhang, and F. Wang, Signatures of tunable superconductivity in a trilayer graphene moiré superlattice, Nature (London) **572**, 215 (2019).

[10] J. M. Park, Y. Cao, K. Watanabe, T. Taniguchi, and P. Jarillo-Herrero, Tunable strongly coupled superconductivity in magic-angle twisted trilayer graphene, Nature (London) **590**, 249 (2021).

[11] H. Zhou, T. Xie, T. Taniguchi, K. Watanabe, and A. Young, Superconductivity in rhombohedral trilayer graphene, Nature (London) **598**, 434 (2021).

[12] Y. Nakagawa, Y. Kasahara, T. Nomoto, R. Arita, T. Nojima, and Y. Iwasa, Gate-controlled BCS-BEC crossover in a two-dimensional superconductor, Science **372**, 190 (2021).

[13] B. K. Chakraverty, J. Ranninger, and D. Feinberg, Experimental and theoretical constraints of bipolaronic superconductivity in high T_c materials: An impossibility, Phys. Rev. Lett. **81**, 433 (1998).

[14] S. A Kivelson, Physics of superconducting transition temperatures, J. Supercond. Nov. Magn. **33**, 5 (2020).

[15] C. Zhang, J. Sous, D. R. Reichman, M. Berciu, A. J. Millis, N. V. Prokof'ev, and B. V. Svistunov, Bipolaronic high-temperature superconductivity, Phys. Rev. X **13**, 011010 (2023).

[16] J. Sous, M. Chakraborty, R. V. Krems, and M. Berciu, Light bipolarons stabilized by Peierls electron-phonon coupling, Phys. Rev. Lett. **121**, 247001 (2018).

[17] C. Zhang, N. V. Prokof'ev, and B. V. Svistunov, Bond bipolarons: Sign-free Monte Carlo approach, Phys. Rev. B **105**, L020501 (2022).

[18] X. Zhou, W.-S. Lee, M. Imada, N. Trivedi, P. Phillips, H.-Y. Kee, P. Törmä, and M. Eremets, High-temperature superconductivity, Nat. Rev. Phys. **3**, 462 (2021).

[19] K. Slagle and L. Fu, Charge transfer excitations, pair density waves, and superconductivity in moiré materials, Phys. Rev. B **102**, 235423 (2020).

[20] V. Crépel and L. Fu, New mechanism and exact theory of superconductivity from strong repulsive interaction, Sci. Adv. **7**, eabh2233 (2021).

[21] V. Crépel, T. Cea, L. Fu, and F. Guinea, Unconventional superconductivity due to interband polarization, Phys. Rev. B **105**, 094506 (2022).

[22] V. Crépel and L. Fu, Spin-triplet superconductivity from excitonic effect in doped insulators, Proc. Natl. Acad. Sci. USA **119**, e2117735119 (2022).

[23] A. S. Alexandrov, Polaron dynamics and bipolaron condensation in cuprates, Phys. Rev. B **61**, 12315 (2000).

[24] J. P. Hague, P. E. Kornilovitch, J. H. Samson, and A. S. Alexandrov, Superlight small bipolarons in the presence of a strong Coulomb repulsion, Phys. Rev. Lett. **98**, 037002 (2007).

[25] S. Barišić, J. Labbé, and J. Friedel, Tight binding and transition-metal superconductivity, Phys. Rev. Lett. **25**, 919 (1970).

[26] W. P. Su, J. R. Schrieffer, and A. J. Heeger, Solitons in polyacetylene, Phys. Rev. Lett. **42**, 1698 (1979).

[27] M. Capone, W. Stephan, and M. Grilli, Small-polaron formation and optical absorption in Su-Schrieffer-Heeger and Holstein models, Phys. Rev. B **56**, 4484 (1997).

[28] C. A. Perroni, E. Piegari, M. Capone, and V. Cataudella, Polaron formation for nonlocal electron-phonon coupling: A variational wave-function study, Phys. Rev. B **69**, 174301 (2004).

[29] D. J. J. Marchand, G. De Filippis, V. Cataudella, M. Berciu, N. Nagaosa, N. V. Prokof'ev, A. S. Mishchenko, and P. C. E. Stamp, Sharp transition for single polarons in the

one-dimensional Su-Schrieffer-Heeger model, Phys. Rev. Lett. **105**, 266605 (2010).
[30] C. Zhang, N. V. Prokof'ev, and B. V. Svistunov, Peierls/Su-Schrieffer-Heeger polarons in two dimensions, Phys. Rev. B **104**, 035143 (2021).
[31] M. R. Carbone, A. J. Millis, D. R. Reichman, and J. Sous, Bond-Peierls polaron: Moderate mass enhancement and current-carrying ground state, Phys. Rev. B **104**, L140307 (2021).
[32] N. V. Prokof'ev and B. V. Svistunov, Phonon modulated hopping polarons: x-representation technique, Phys. Rev. B **106**, L041117 (2022).
[33] B. Xing, W.-T. Chiu, D. Poletti, R. T. Scalettar, and G. Batrouni, Quantum Monte Carlo simulations of the 2D Su-Schrieffer-Heeger model, Phys. Rev. Lett. **126**, 017601 (2021).
[34] X. Cai, Z.-X. Li, and H. Yao, Antiferromagnetism induced by bond Su-Schrieffer-Heeger electron-phonon coupling: A quantum Monte Carlo study, Phys. Rev. Lett. **127**, 247203 (2021).
[35] A. Götz, S. Beyl, M. Hohenadler, and F. F. Assaad, Valence-bond solid to antiferromagnet transition in the two-dimensional Su-Schrieffer-Heeger model by Langevin dynamics, Phys. Rev. B **105**, 085151 (2022).
[36] X. Cai, Z.-X. Li, and H. Yao, Robustness of antiferromagnetism in the Su-Schrieffer-Heeger Hubbard model, Phys. Rev. B **106**, L081115 (2022).
[37] C. Feng, B. Xing, D. Poletti, R. Scalettar, and G. Batrouni, Phase diagram of the Su-Schrieffer-Heeger-Hubbard model on a square lattice, Phys. Rev. B **106**, L081114 (2022).
[38] A. Nocera, J. Sous, A. E. Feiguin, and M. Berciu, Bipolaron liquids at strong Peierls electron-phonon couplings, Phys. Rev. B **104**, L201109 (2021).
[39] B. Spivak and S. A. Kivelson, Phases intermediate between a two-dimensional electron liquid and Wigner crystal, Phys. Rev. B **70**, 155114 (2004).
[40] C. Zhang, B. Capogrosso-Sansone, M. Boninsegni, N. V. Prokof'ev, and B. V. Svistunov, Superconducting transition temperature of the Bose one-component plasma, Phys. Rev. Lett. **130**, 236001 (2023).
[41] J. Bonča, T. Katrasňik, and S. A. Trugman, Mobile bipolaron, Phys. Rev. Lett. **84**, 3153 (2000).
[42] A. Macridin, G. A. Sawatzky, and M. Jarrell, Two-dimensional Hubbard-Holstein bipolaron, Phys. Rev. B **69**, 245111 (2004).
[43] W. L. McMillan, Transition temperature of strong-coupled superconductors, Phys. Rev. **167**, 331 (1968).
[44] B. K. Chakraverty, Possibility of insulator to superconductor phase transition, J. Phys. Lett. **40**, 99 (1979).
[45] R. T. Scalettar, N. E. Bickers, and D. J. Scalapino, Competition of pairing and Peierls–charge-density-wave correlations in a two-dimensional electron-phonon model, Phys. Rev. B **40**, 197 (1989).
[46] F. Marsiglio, Pairing and charge-density-wave correlations in the Holstein model at half-filling, Phys. Rev. B **42**, 2416 (1990).
[47] A. S. Alexandrov, Breakdown of the Migdal-Eliashberg theory in the strong-coupling adiabatic regime, Europhys. Lett. **56**, 92 (2001).
[48] J. E. Moussa and M. L. Cohen, Two bounds on the maximum phonon-mediated superconducting transition temperature, Phys. Rev. B **74**, 094520 (2006).
[49] P. Werner and A. J. Millis, Efficient dynamical mean field simulation of the Holstein-Hubbard model, Phys. Rev. Lett. **99**, 146404 (2007).
[50] I. Esterlis, B. Nosarzewski, E. W. Huang, B. Moritz, T. P. Devereaux, D. J. Scalapino, and S. A. Kivelson, Breakdown of the Migdal-Eliashberg theory: A determinant quantum Monte Carlo study, Phys. Rev. B **97**, 140501(R) (2018).
[51] I. Esterlis, S. A. Kivelson, and D. J. Scalapino, A bound on the superconducting transition temperature, npj Quantum Mater. **3**, 59 (2018).
[52] B. Nosarzewski, E. W. Huang, Philip M. Dee, I. Esterlis, B. Moritz, S. A. Kivelson, S. Johnston, and T. P. Devereaux, Superconductivity, charge density waves, and bipolarons in the Holstein model, Phys. Rev. B **103**, 235156 (2021).
[53] R. T. Clay and D. Roy, Superconductivity due to cooperation of electron-electron and electron-phonon interactions at quarter filling, Phys. Rev. Res. **2**, 023006 (2020).
[54] Q.-G. Yang, D. Wang, and Q.-H. Wang, A functional renormalization group study of the two dimensional Su-Schrieffer-Heeger-Hubbard model, Phys. Rev. B **106**, 245136 (2022).
[55] E. Burovski, N. Prokof'ev, B. Svistunov, and M. Troyer, Critical temperature and thermodynamics of attractive fermions at unitarity, Phys. Rev. Lett. **96**, 160402 (2006).
[56] E. Burovski, N. Prokof'ev, B. Svistunov, and M. Troyer, The Fermi–Hubbard model at unitarity, New J. Phys. **8**, 153 (2006).